Journal of Photochemistry & Photobiology, B: Biology 164 (2016) 174–181

Contents lists available at ScienceDirect

Journal of Photochemistry & Photobiology, B: Biology

journal homepage: www.elsevier.com/locate/jphotobiol

Toxicity and efficacy of CdO nanostructures on the MDCK and Caki-2 cells

T.V.M. Sreekanth [a,1], Muthuraman Pandurangan [b,1], G.R. Dillip [c], Doo Hwan Kim [b], Yong Rok Lee [a,*]

[a] Department of Chemical Engineering, Yeungnam University, Gyeongsan-38541, Republic of Korea
[b] Deptartment of Bioresources and Food Science, Konkuk University, Seoul-05029, Republic of Korea
[c] School of Mechanical Engineering, Yeungnam University, Gyeongsan-38541, Republic of Korea

ARTICLE INFO

Article history:
Received 17 August 2016
Received in revised form 19 September 2016
Accepted 21 September 2016
Available online 23 September 2016

Keywords:
Green synthesis
CdO nanostructures
XPS
Cell viability
Tumor cells

ABSTRACT

This article reports the toxicological effects of synthesized cadmium oxide (CdO) nanostructures via a simple green route using a *Polygala tenuifolia* root extract on normal and renal tumor cells. First, the formation of cadmium oxide nanostructures were confirmed structurally by Fourier transform infrared spectroscopy, X-ray diffraction, and X-ray photoelectron spectroscopy (XPS). The powder was crystallized in a cubic structure with a space group of *Fm*-3*m*. The mean crystallize size was approximately 40 and 44 nm from the Scherrer and size-strain plots, respectively. The surface states of the cadmium oxide nanostructure using the O 1s and Cd 3d spectra were analyzed by XPS. Transmission electron microscopy showed that the simple green route resulted in various morphologies of synthesized cadmium oxide, such as trigonal-, tetrahedron-, and sheet-like structures. Finally, the toxic effects of the cadmium oxide nanostructures on Madin-Darby canine kidney epithelial cells (MDCK cells), as well as the human renal cancer cell line (Caki-2 cells) were investigated using a SRB assay and two-color flow cytometry analysis. The cadmium oxide nanostructures showed significant cell growth inhibition in normal and also tumor cells in a dose-dependent manner. On the other hand, the inhibition was higher in the cancer cells compared to the normal cells.

1. Introduction

Currently, there is increasing interest in the bulk production of nanomaterials for use in several commercial products because of their novel and unique physicochemical properties [1]. Various properties of materials, such as electrical conductivity, magnetic characteristics, hardness, active surface area, chemical reactivity, and biological activity, can be altered during the change from the macro to nano-dimensions. Because of these enhanced characteristics, nanomaterials have been used extensively in several scientific and technological areas. Over the past few years, advances in nanotechnology and nanomedicine, the use of these materials have increased in many biomedical applications, such as bio-imaging, controlled drug release, and cancer treatment [2]. In addition to biomedical applications, these nanomaterials are used commercially in products, such as clothes, sunscreens, cosmetics, electronics, food color additives, surfaces, and coatings [3]. The widespread use of nanoparticles has led to an increased exposure and subsequent toxicity to humans, making it imperative to study their toxicological effects and long-term impacts on health. The toxic effects of nanoparticles are influenced by the size, shape, surface structure, solubility, chemical composition crystallinity, and aggregation [4]. In biological systems, these factors regulate the cellular uptake, protein binding, translocation into the target cell and the possibility of causing tissue injury [5]. Nanoparticles below 100 nm in size easily enter the cells, whereas those below 40 nm easily penetrate the nucleus, and below 35 nm, can even pass the blood-brain barrier [6].

Few studies have reported the effects of nanoparticles on the kidneys; both glomerular structures during plasma ultra-filtration and tubular epithelial cells may be exposed to nanoparticles [7]. For example, Chen et al. [8] observed damage to the proximal tubular cells in mice exposed to CuNPs. Karlsson et al. [9] synthesized and investigated whether nanoparticles cause DNA damage and oxidative stress. They also carried out a comparative cytotoxicity study on different metal oxides (CuO, TiO_2, ZnO, $CuZnFe_2O_4$, Fe_3O_4, Fe_2O_3), and carbon nanoparticles/nanotubes. Hossain and Mukherjee [10]reported the results of a toxicological study of CdO nanoparticles on *Escherichia coli*. On the other hand, reports on the toxic effects of CdO nanoparticles are limited.

Cadmium oxide (CdO), a II-VI *n*-type semiconductor, has outstanding properties, such as a large band gap, low electrical resistivity, and high transmission in the visible region. Based on these properties, CdO has been used in applications, such as solar cells [11], transparent electrodes, gas sensors [12], phototransistors [13], catalysts [14], photodiodes [15], optoelectronic devices [16], drug delivery [17], and targeted therapeutics. This has warranted the massive production of engineered CdO nanoparticles/quantum dots, resulting in the massive release of nano-sized Cd particles into the environment. Owing to its higher

* Corresponding author.
E-mail address: yrlee@yu.ac.kr (Y.R. Lee).
[1] Authors contributed equally to this work.

http://dx.doi.org/10.1016/j.jphotobiol.2016.09.028
1011-1344/

surface area to volume ratio, the toxicity of Cd nanoparticles causes significant damage to biological systems.

This study examined the toxic effects of CdO nanostructures on MDCK and Caki-2 cells. The CdO nanostructures were synthesized by a simple inexpensive and non-toxic method using a plant extract. This method involves less toxic chemicals, and is eco-friendly physical and chemical process. This study tested whether the prepared nanostructures have potential toxicity to cells. This paper deals with two parts. The first part describes the synthesis, structural and morphological properties of the CdO nanostructures, and the second part reports the effects of these nanostructures on the cell viability of MDCK and Caki-2 cells.

2. Materials and Methods

2.1. Chemicals

All chemicals and reagents used in this study were of high purity (99.9%) and used as received. Cadmium acetate dihydrate [$Cd(CH_3COO)_2 \cdot 2H_2O$], dimethyl sulphoxide (DMSO) and sulforhodamine B (SRB) were purchased from Sigma-Aldrich Pvt. Ltd., South Korea. DMEM, FBS, penicillin-streptomycin, and trypsin-EDTA were obtained from Welgene, South Korea. Fluorescein diacetate (FDA) and propidium iodide (PI) were supplied by Santa Cruz Biotechnology, USA.

2.2. Cell Culture

MDCK and Caki-2 cells were obtained from the ATCC (Manassas, VA 20108 USA). The cells were kept in the growth medium supplemented with 10% FBS and 1% antibiotics (penicillin-streptomycin). The cells were maintained in a CO_2 incubator under standard conditions (37 °C and 5% CO_2).

2.3. Green Synthesis of CdO Nanostructures

Polygala tenuifolia roots were collected from an oriental supermarket, Gyeongsan, South Korea. The CdO nanostructures were synthesized as reported elsewhere [18]. Approximately 10 g of the finely ground root powder was added to 100 ml of de-ionized (DI) water, heated to 80 °C for 45 min and filtered through Whatman no: 42 filter paper. To this extract, 2.66 g of cadmium acetate was added and stirred at room temperature for 20 min for complete dissolution. Subsequently, the temperature was increased to 120 °C for 4 h. After cooling to room temperature, a fine white precipitate was observed at the bottom of the round bottom flask, which was separated by centrifugation at 12,000 rpm for 15 min. This was repeated 3–4 times to remove the unreacted materials and finally washed with ethanol. The precipitate was collected, dried in an oven at 60 °C for 2 h, and annealed in a muffle furnace at 500 °C for 4 h. The resulting nanopowder was used for various characterizations.

2.4. Characterization

The CdO nanostructure was pelletized with KBr and examined by Fourier transform infrared spectroscopy (FT-IR, Perkin-Elmer-Spectrum Two). The polycrystalline nature of the sample was examined by X-ray diffraction (XRD, PANalytical X'Pert^3 PRO, USA) using Cu K_α radiation ($\lambda = 1.54$ Å) at 40 kV and 30 mA. Energy dispersive X-ray spectroscopy (EDAX) was performed using an X-ray column attached to the field emission-scanning electron microscope (FE-SEM, Hitachi-4200, Japan). The surface states of the CdO nanostructure were studied by X-ray photoelectron spectroscopy (XPS, Thermo Scientific K-Alpha)

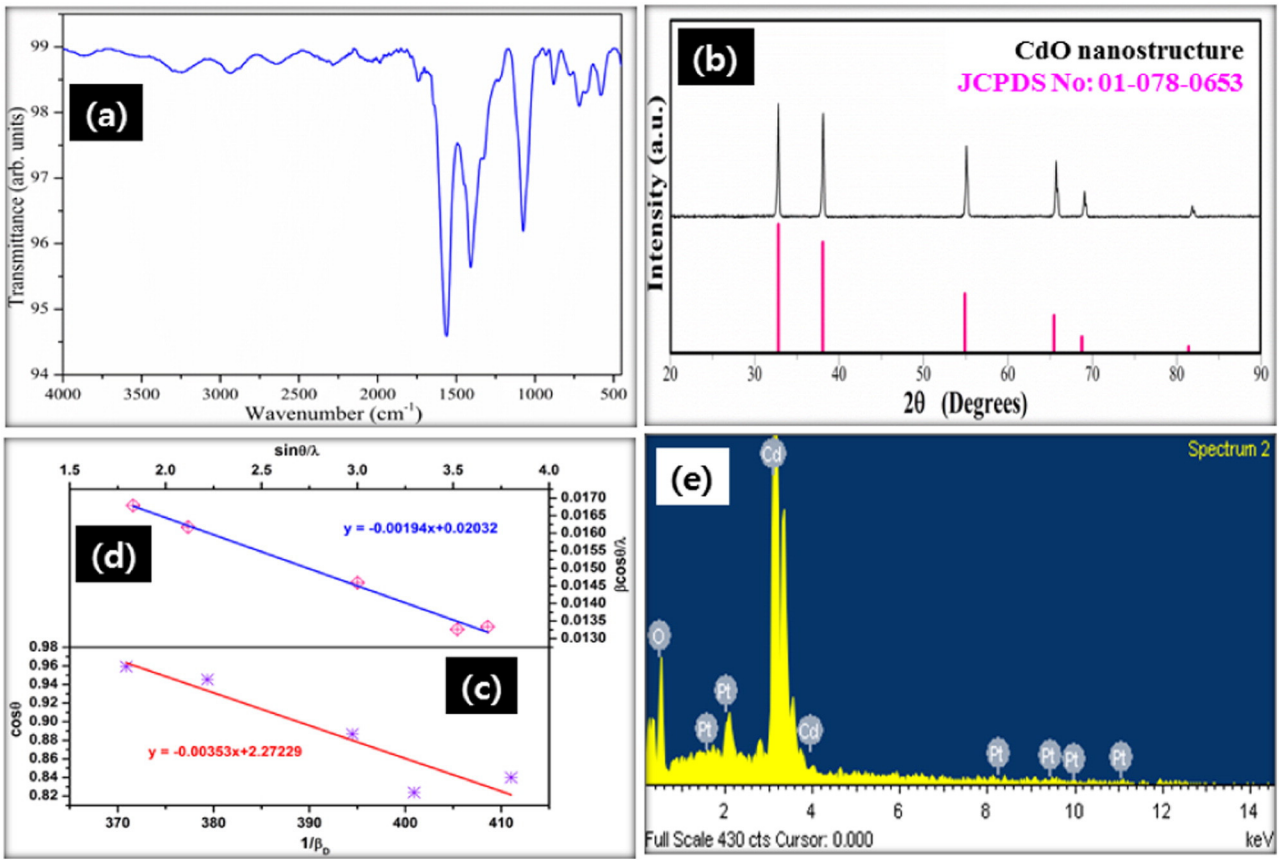

Fig. 1. FT-IR spectrum a), XRD pattern b), plots of cos θ versus $1/\beta_D$ c) and size-strain d), and EDAX profile e) of green synthesized nanostructures.

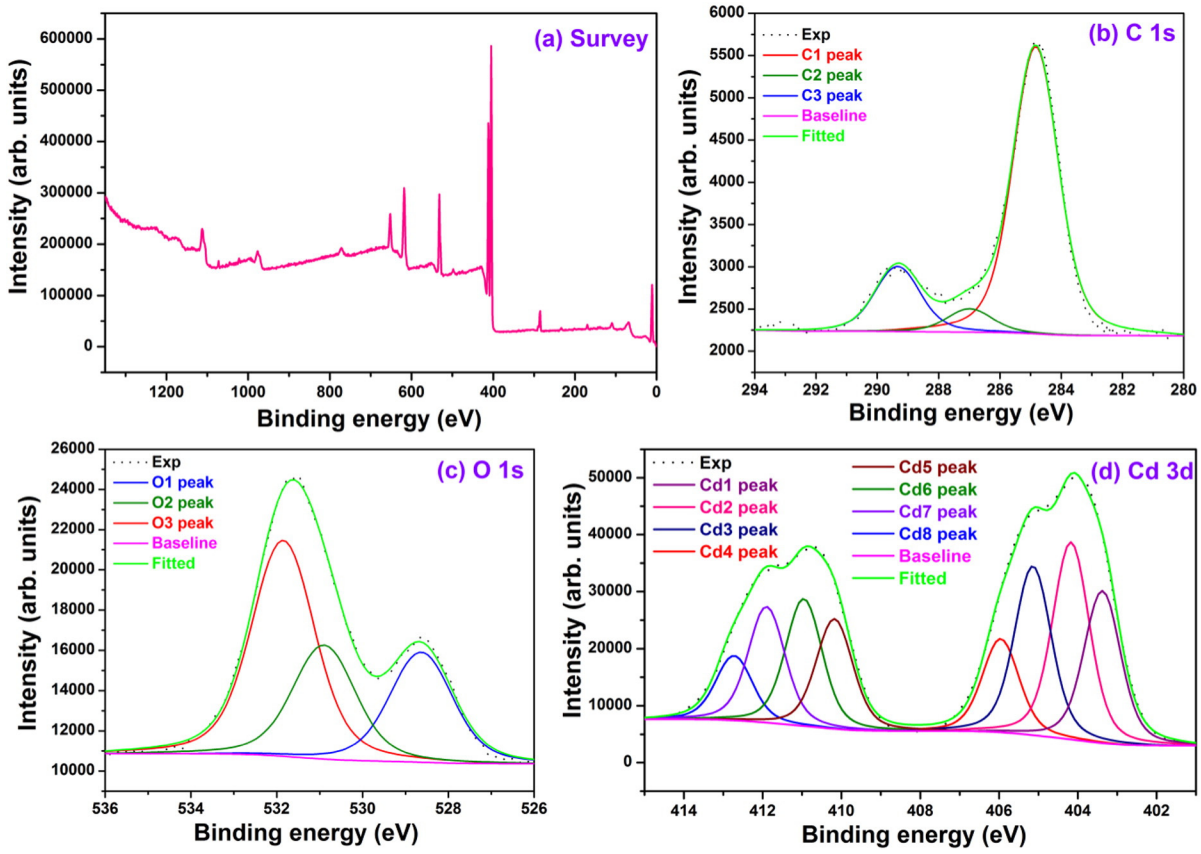

Fig. 2. XPS analysis of green synthesized nanostructures: survey scan a) and high-resolution scans of C 1s b), O 1s c), and Cd 3d d).

using a monochromatic Al K_α X-ray source (1486.6 eV). The source energies of 160 eV and 30 eV with a resolution of 1 and 0.1 eV were used for the low and high-resolution scans, respectively. The morphology of the green synthesized CdO nanostructures was observed by high-resolution transmission electron microscopy (HR-TEM, Tecnai G2 F20 S-Twin, USA) operating at an accelerating voltage of 200 kV with a point resolution of 0.24 nm and a Cs of 1.2 mm. To prepare the sample, a small amount of powder was dispersed in water, sonicated for 5 min and drop-coated on a commercially available carbon-coated copper grid. The grid was dried under visible-light for 10 min. The length scales are indicated systematically as a black bar on the bottom corner of the images.

2.5. Cell Viability Assay

MDCK and Caki-2 cells were cultured and grown in 96-well plates and allowed to adhere for 24 h at 37 °C. The cells were treated with CdO nanostructures at different concentrations (10 μg/ml, 100 μg/ml, 1 mg/ml, and 10 mg/ml) for 48 h, after which the cell viability was determined, as described previously [19].

2.6. Two-color Flow Cytometric Analysis of Apoptosis

The MDCK and Caki-2 cells were cultured and grown to a density of 2×10^4 cells/well in 6-well plates. The cells were allowed 24 h to adhere and were then treated with the CdO nanostructures at different concentrations (100 μg/ml, 1 mg/ml, and 10 mg/ml) for 48 h. The cells were then washed with PBS and re-suspended in PBS at an initial cell density of 1×10^4 cells/ml. FDA was added to each tube to reach a final concentration of 0.5 μg/ml and the tubes were incubated in the dark for 30 min. Subsequently, PI was added to each tube to achieve a final concentration of 50 μg/ml. All the tubes were kept on ice immediately until analyzed by flow cytometry [20].

The cell viability was assessed by determining the intracellular green and red fluorescence using a BD FACS Calibur Flow Cytometry System (Becton Dickinson, Franklin Lakes, NJ 07417). A 570-nm beam splitter was used for dual color fluorescence analysis, a 625-nm filter used to collect the red (PI) fluorescence, and a 530-nm filter was used for green (FDA) fluorescence. The logarithmic amplification of the red and green fluorescence signals was used. High green fluorescence indicates the viable cells.

3. Results and Discussion

FT-IR analysis was carried out to identify the biomolecules responsible for the formation of CdO nanostructures. Fig. 1a presents a typical FT-IR spectrum of CdO nanostructures. The spectrum was composed of several significant peaks at 1564, 1405, 1074, 881, and 717 cm^{-1}. The metallic bonds observed near the 881 cm^{-1} is due to metal–hydroxide (M—OH), whereas the band identified at 717 cm^{-1} is due to metal-oxygen bond (M—O) [21]. The absorption peak at 1074 cm^{-1} corresponds to the —OCH_3 group, which is arises due to the carbon species from the root extract [22]. FT-IR spectroscopy confirmed that cadmium and oxygen are present in the range between 1641 and 1270 cm^{-1} [23].

To determine the crystallographic structure of the green-synthesized CdO nanostructures, XRD was performed over the 2θ range, 20–90°. Fig. 1b shows the typical XRD pattern of the highly crystallized CdO nanostructures. The profile shows six distinct Bragg peaks with a high degree of symmetry, all of which were well matched with Joint Committee on Powder Diffraction Standards (JCPDS) card no: 01–078-0653. The powder was crystallized in a cubic structure with *Fm*-3*m*

Table 1
XPS analysis of green synthesized CdO nanostructures.

Region	Peak	Position BE (eV) ±0.1	FWHM (eV)±0.1	Raw area (cps)	Relative at%	Elemental at%
C 1s	C1	284.8	1.75	6977.3	19.26	25.23
	C2	287.0	1.75	572.1	1.58	
	C3	289.3	1.75	1585.6	4.39	
O 1s	O1	528.6	1.73	11,055.3	12.59	50.57
	O2	530.9	1.73	11,500.4	13.12	
	O3	531.9	1.73	21,771.3	24.86	
Cd 3d	Cd1	403.4	1.10	34,321.3	3.54	24.20
	Cd2	404.2	1.10	44,611.6	4.06	
	Cd3	405.1	1.10	38,207.8	3.94	
	Cd4	406.0	1.10	21,120.4	3.83	
	Cd5	410.2	1.10	24,857.6	2.57	
	Cd6	411.0	1.10	28,755.9	2.98	
	Cd7	411.9	1.10	26,209.3	2.72	
	Cd8	412.7	1.10	14,616.4	–	

space group. The peaks centered at 32.80, 38.06, 54.91, 65.76, 68.77, and 81.40° were assigned to the (111), (200), (220), (311), (222) and (400) lattice-planes, respectively. The XRD pattern was refined using celref 3 software provided by collaborative computational project number 14 (CCP14). The lattice constants of $a = 0.47306$ nm and volume of 0.105866 nm^3 were obtained. These values are in line with the JCPDS data. The mean crystallite size of the CdO nanostructures was calculated using the X-ray peak broadening method by plotting the Scherrer and size-strain plots. The formulae and method used to calculate the crystallite size is reported in elsewhere [24,25]. The plots of $\frac{1}{\beta_D}$(x-axis) vs. cos θ (y-axis) (Fig. 1(c)) and sinθ/λ vs. βcosθ/λ (Fig. 1(d)) were fitted to linear functions. The crystalline size was calculated from the slope of the fits. The mean crystallite sizes of the CdO nanostructures were determined to be 40 and 44 nm from Scherrer and size-strain plots, respectively. The order of these values was consistent with the mean grain-sizes determined from the HR-TEM images.

Fig. 1(e) presents the corresponding elemental profile of the CdO nanostructures. The profile shows the significant peaks for cadmium (Cd) (3.20 and 3.80 eV) and oxygen (O) (0.60 eV) and platinum (Pt), which are at various energy channels, as indexed in the figure. The Cd and O peaks were attributed to the synthesized nanostructure. On the other hand, the Pt peak originated from the thin layer of sputtered Pt onto the film to minimize the charge build up from the electrons during the SEM measurements.

XPS was carried out to investigate the nature of the elements on the surface, their percentage composition, and the chemical state of the nanostructure. Fig. 2(a) shows the signals of the C 1s, O 1s, and Cd 3d without other impurities. To study the bonding of these elements in detail, the core-level spectra of C 1s, O 1s, and Cd 3d were recorded and deconvoluted using Avantage software. The Shirley background and Gaussian (70%)-Lorentz (30%) (GL = 30) function were used to fit the spectra. The fitting was done by keeping the full-width-half-maxima (FWHM) values as constant for each element. The spectra were energy corrected for all elements by referring to the adventitious carbon binding energy, 284.8 eV, these results were tabulated in Table 1.

The deconvoluted C 1s spectrum showed three peaks at C1: 284.8 eV, C2: 287.0 eV, and C3: 289.3 eV (Fig. 2b). The peaks at 284.8 eV and 289.3 eV were in good accordance with values for aliphatic carbon and carboxyl carbon, respectively. This also corroborates the FT-IR values. This suggests that the CdO nanostructures surfaces were coordinated with biomass materials, which is also seen in the HR-TEM image (Fig. 3a). These peaks originated from the two sources: one from carbon containing biomass material of the plant extract and the other to the

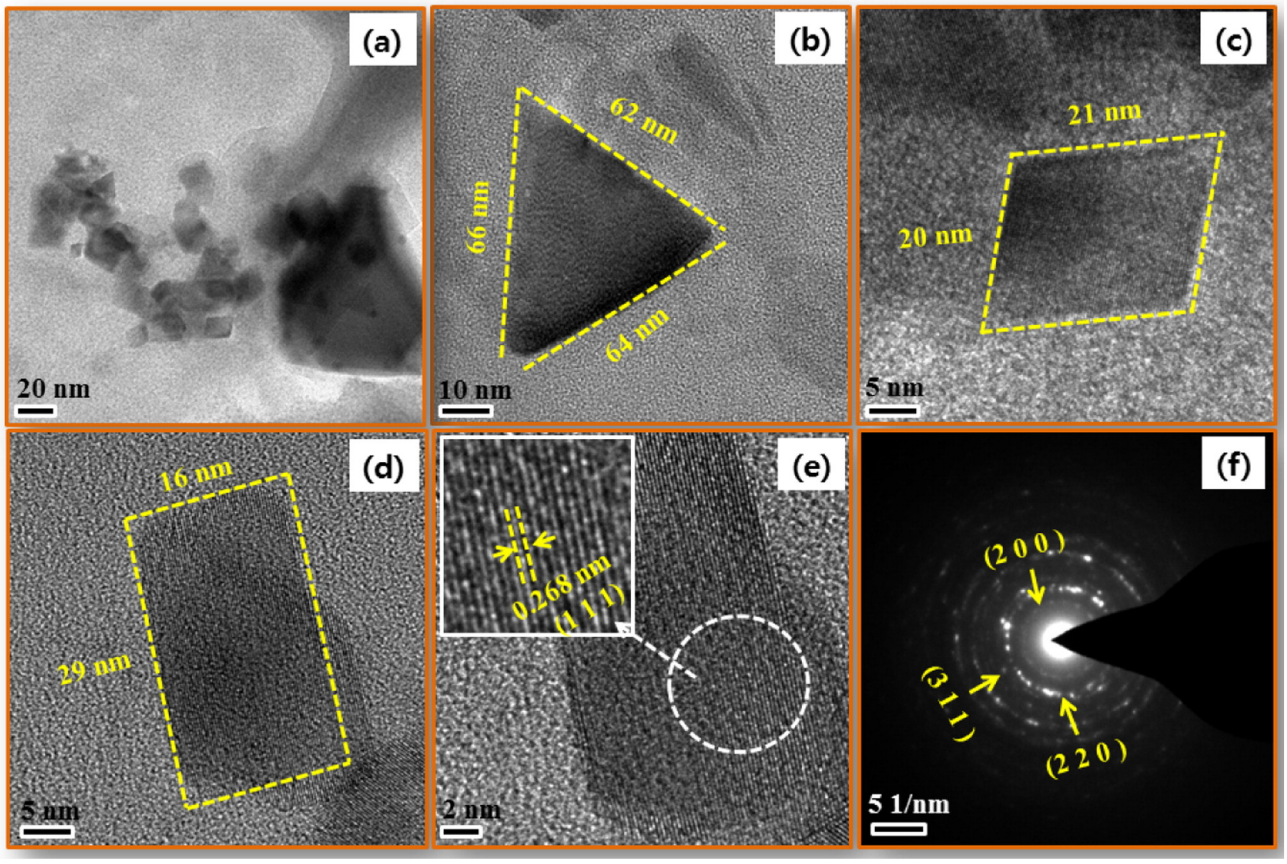

Fig. 3. TEM a), HRTEM images of trigonal-like b), tetrahedron-like c), and rectangular sheet-like nanostructures d) and corresponding high-magnification HRTEM e), and SAED pattern f) of CdO nanostructures.

adsorption of carbon on the sample surface during sample preparation at ambient atmosphere [26].

Fig. 2(c) shows a high-resolution XPS spectrum of O 1s. The spectrum is composed of three peaks at O1: 528.6 eV, O2: 530.9 eV, and O3: 531.9 eV [27]. The lower binding energy peak at 528.6 eV corresponds to the bonding of O^{2-} with Cd^{2+} ions in stoichiometric CdO [28]. The higher binding energy peak at 531.9 eV was assigned to hydroxyl oxygen on the surface, and the peak at 530.9 eV is due to the presence of CdO_x sub-oxides.

The Cd 3d high resolution spectrum showed two asymmetric peaks at 404.0 and 410.7 eV, which were assigned to the spin-orbit splitting of Cd $3d_{5/2}$ and $3d_{3/2}$, respectively. The $3d_{5/2}$ and $3d_{3/2}$ spin-orbit separation of 6.7 eV was obtained. The characteristic binding energy of Cd $3d_{5/2}$ and $3d_{3/2}$ were good agreement with that of CdO nanostructures reported in the literature [29]. Each of the asymmetric peaks was further deconvoluted into four symmetrical peaks with an equal FWHM, as shown in Fig. 2(d). This suggests the different boding environment of Cd in CdO nanostructures. The peak couples at 403.4/410.2 eV, 404.2/411.0 eV, 405.1/411.9 eV, and 406.0/412.7 eV were assigned to the spin-orbit splitting of Cd $3d_{5/2}$ and $3d_{3/2}$ for CdO_x, CdO, $Cd(OH)_2$, and $CdCO_3$, respectively. The CdO_x and $Cd(OH)_2$peaks were attributed to the partial transformation of CdO nanostructures during sample preparation under ambient conditions for the XPS measurement. The $CdCO_3$ peak was attributed to adsorbed carbon species from atmosphere as well as a carbon containing plant extract. These bands were also observed in the high-resolution scan of C 1s and O 1s [30,31].

HR-TEM analysis was carried out to examine the morphology and size of green-synthesized CdO nanostructures. Fig. 3(a) shows a typical low-magnification HR-TEM image. The nanostructure of CdO is unclear from the images; however, the aggregations of particles are much less. A careful look certainly indicates that CdO was formed by various morphologies in the range, 20 to 70 nm. To corroborate this, high-magnification HR-TEM images were recorded, as shown in Fig. 3(b–e). The morphology of CdO has trigonal-like (adjacent sides of ~64 nm, Fig. 3(b)), tetrahedron-like (adjacent sides of ~20 nm, Fig. 3(c)), and rectangular sheet-like structures (adjacent sides of ~16 nm × 29 nm, Fig. 3(d)), as indicated in the respective figures. The grain-size of these shapes is in the order of the crystallite sizes, which were estimated by XRD. The high-magnification HR-TEM image (Fig. 3(e)) revealed a d-spacing of 0.268 nm for the (111) direction, which is consistent with the d-spacing from the XRD peak. Fig. 3(f) shows the SAED pattern of the CdO nanostructure. This shows the poly-crystalline nature of the sample and the lattice planes were well matched with the CdO crystal. HR-TEM suggests that the nanostructure of CdO is formed by a variety of shapes in the range of 20 to 70 nm, which can be used to study the cytotoxicity of cells.

The CdO nanostructures had a significant cytotoxic effect on the MDCK and Caki-2 cells. Exposure of MDCK cells to the CdO nanostructures resulted in 3.21%, 24.17%, 42.67%, and 79.55% growth inhibition at 10 μg/ml, 100 μg/ml, 1 mg/ml, and 10 mg/ml respectively, whereas it was 11.8%, 39.44%, 65.36%, and 98.79% in the renal carcinoma cells respectively (Fig. 4).

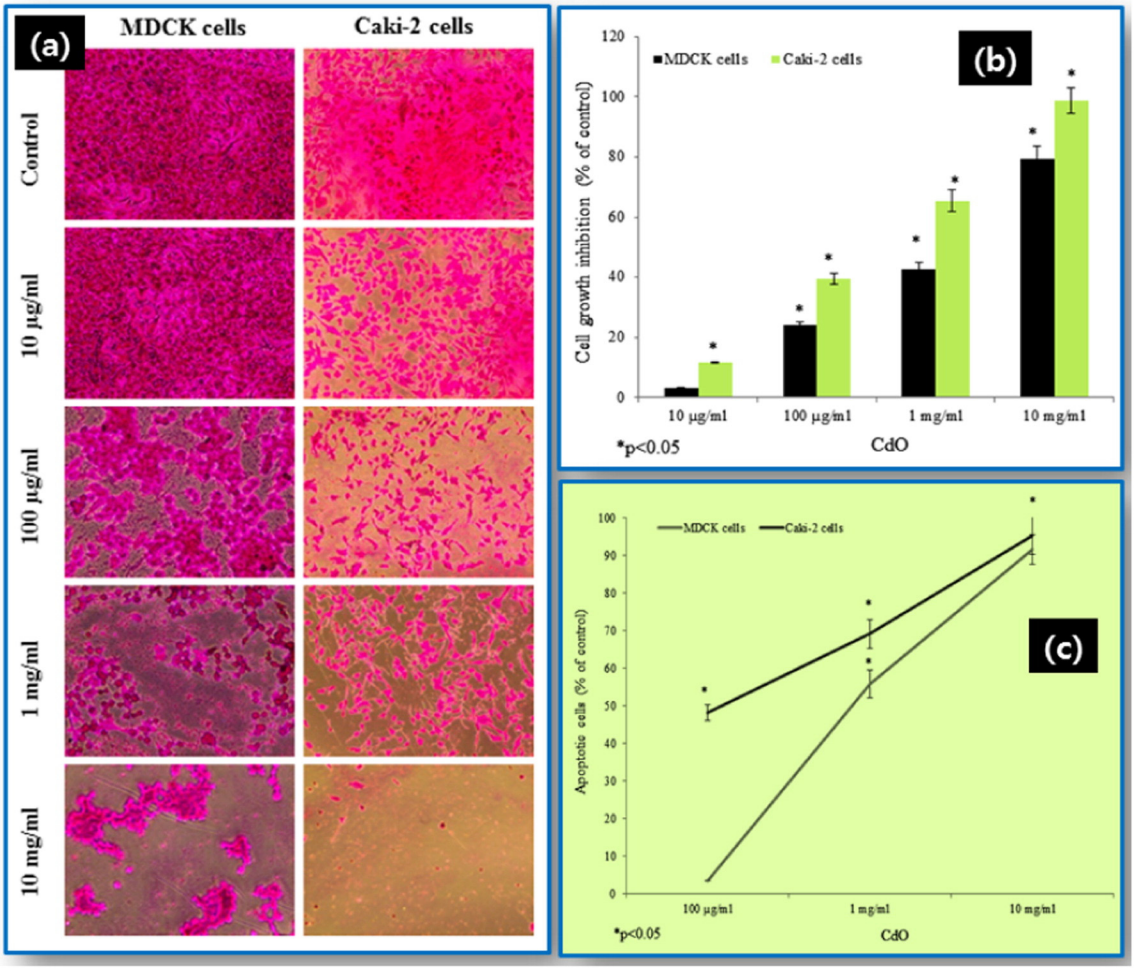

Fig. 4. Cytotoxic effect of CdO nanostructures on MDCK and Caki-2 cells by SRB assay at 48 h a). Results were expressed as a percentage of viability of MDCK and HeLa cells b). The percentage of growth inhibition c) was calculated as follows: Growth inhibition (%): (Control-Sample/Control) × 100. Values were expressed as means ± SEM, and effect of CdO nanostructures on Caki-2 cells determined by FDA and PI (c).

In this study, FDA and PI were used to determine the number of viable and nonviable cells. FDA is a non-polar and non-fluorescent compound. In the viable cells, FDA can enter freely; there it is converted by intracellular esterase into a fluorescent compound. Fluorescein is a highly polar compound, which becomes trapped within the viable cells with an intact membrane. On the other hand, fluorescein diffuses out of the cells, which lacks membrane integrity. Viable cells with FDA appeared as bright green fluorescence, whereas the non-viable cells were non-fluorescent according to flow cytometry analysis. PI is a highly polar and fluorescent substance that can enter the non-viable cells freely where the membrane integrity is absent. Therefore, non-viable cells have bright red fluorescence during flow cytometry analysis. The flow cytometry results are presented in a dot plot on the log scale of green versus red fluorescence. The non-viable cells and debris events are separated from the viable cells in the dot plots, which confirm that the non-viable and cell debris were not counted in the viable cell window. The MDCK and Caki-2 cells were incubated with FDA for 30 min and PI before flow cytometric analysis. A large population of cells showed FDA fluorescence under controlled conditions (area R3 of Figs. 5 and 6), indicating they were intact active living cells.

Exposure to different concentrations of CdO nanostructures for 48 h (100 μg/ml, 1 mg/ml and 10 mg/ml) resulted in very significant cell growth inhibition in MDCK and Caki-3 cells (Figs. 4–6). The number of viable and non-viable cells changed in a dose-dependent manner (Figs. 5 and 6). Exposure to different concentrations of the CdO nanostructures for 48 h inhibited MDCK cell growth. The percentage of non-viable (PI) cells was 3.24%, 75.69%, and 95.60% following exposure to 100 μg/ml, 1 mg/ml, and 10 mg/ml of CdO nanostructures, respectively (area R4 + R5 of Fig. 5). On the other hand, exposure to different concentrations of CdO nanostructures for 48 h inhibited renal tumor cell growth. The percentage of non-viable (PI) cells was 48.24%, 53.16%, and 95.30% following to exposure 100 μg/ml, 1 mg/ml, and 10 mg/ml of CdO nanostructures, respectively (area R4 + R5 of Fig. 6).

The widespread abundance of cadmium can pose a threat to human and animal health. Cd^{2+} is a biologically significant ionic form of cadmium that binds to several bio-molecules; these interactions lead to toxicity. Cadmium toxicity is commonly mediated through biological systems, which amplify the signals triggered in the presence of Cd^{2+}. Cd^{2+} can interfere with sensitive redox systems and act at the transcription and post-transcription levels. A study of the mechanism of cadmium toxicity could be useful for addressing various environmental challenges. In addition, more study will be needed to address the biologically relevant cadmium concentrations on different cell types, and integrate all cellular aspects of the effects of cadmium [32,33].

4. Conclusion

This study is one of the first to investigate the toxic effects of CdO nanostructures on the Human Renal Cancer Cell Line (Caki-2) and Madin-Darby Canine Kidney Epithelial cells (MDCK cells). This paper reported a simple green chemistry approach for the synthesis of CdO nanostructures using the aqueous root extract of *Polygala tenuifolia.*

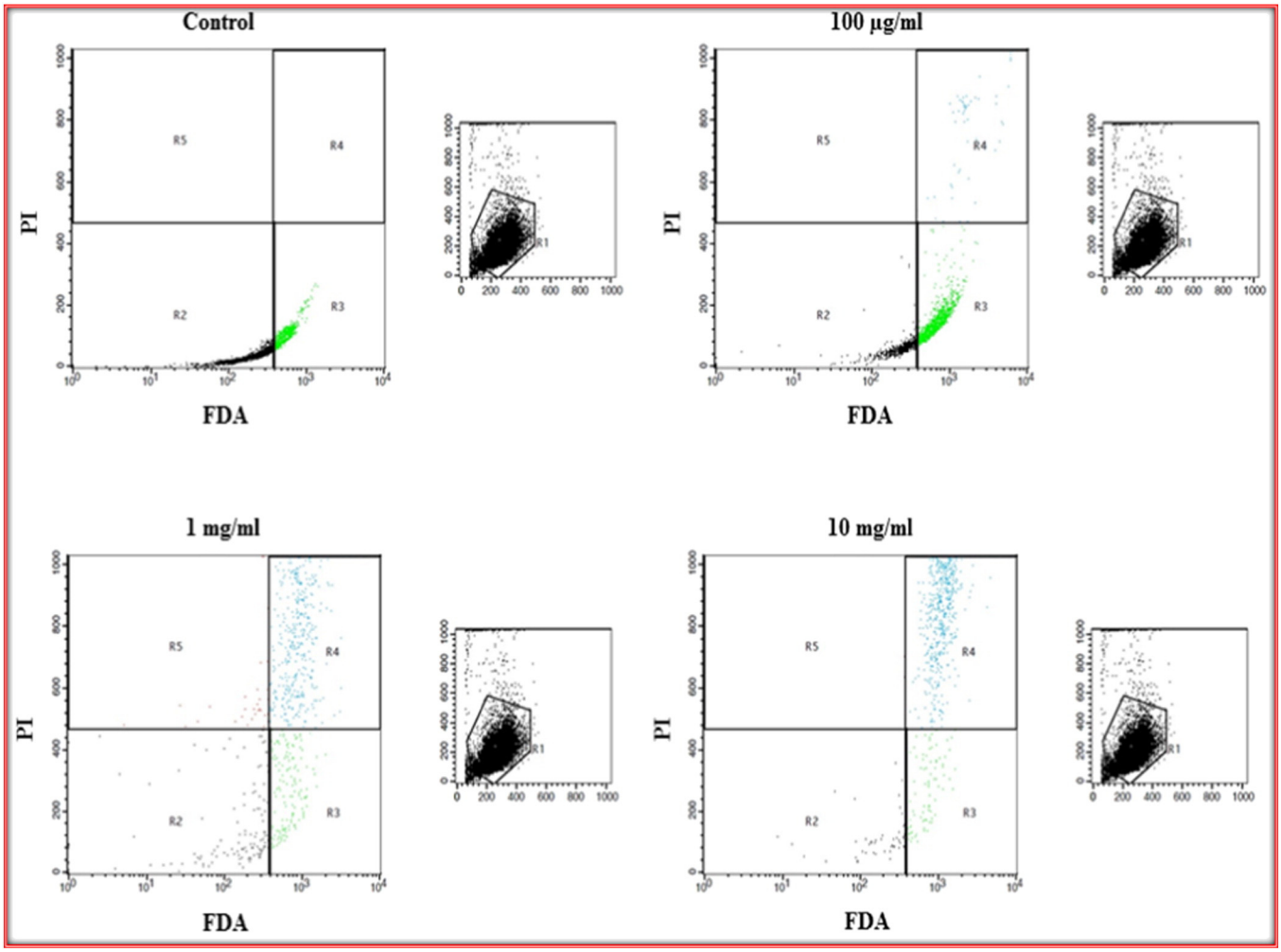

Fig. 5. Effect of CdO nanostructures on MDCK cells were determined by FDA and PI. Area R3 is FDA positive, R5 is PI positive, R4 is both FDA and PI positive, and R2 is both FDA and PI negative. The effect of CdO nanostructures (100 μg/ml, 1 mg/ml and 10 mg/ml) on MDCK cell was examined at 48 h. The percentage of apoptotic cells were calculated (c).

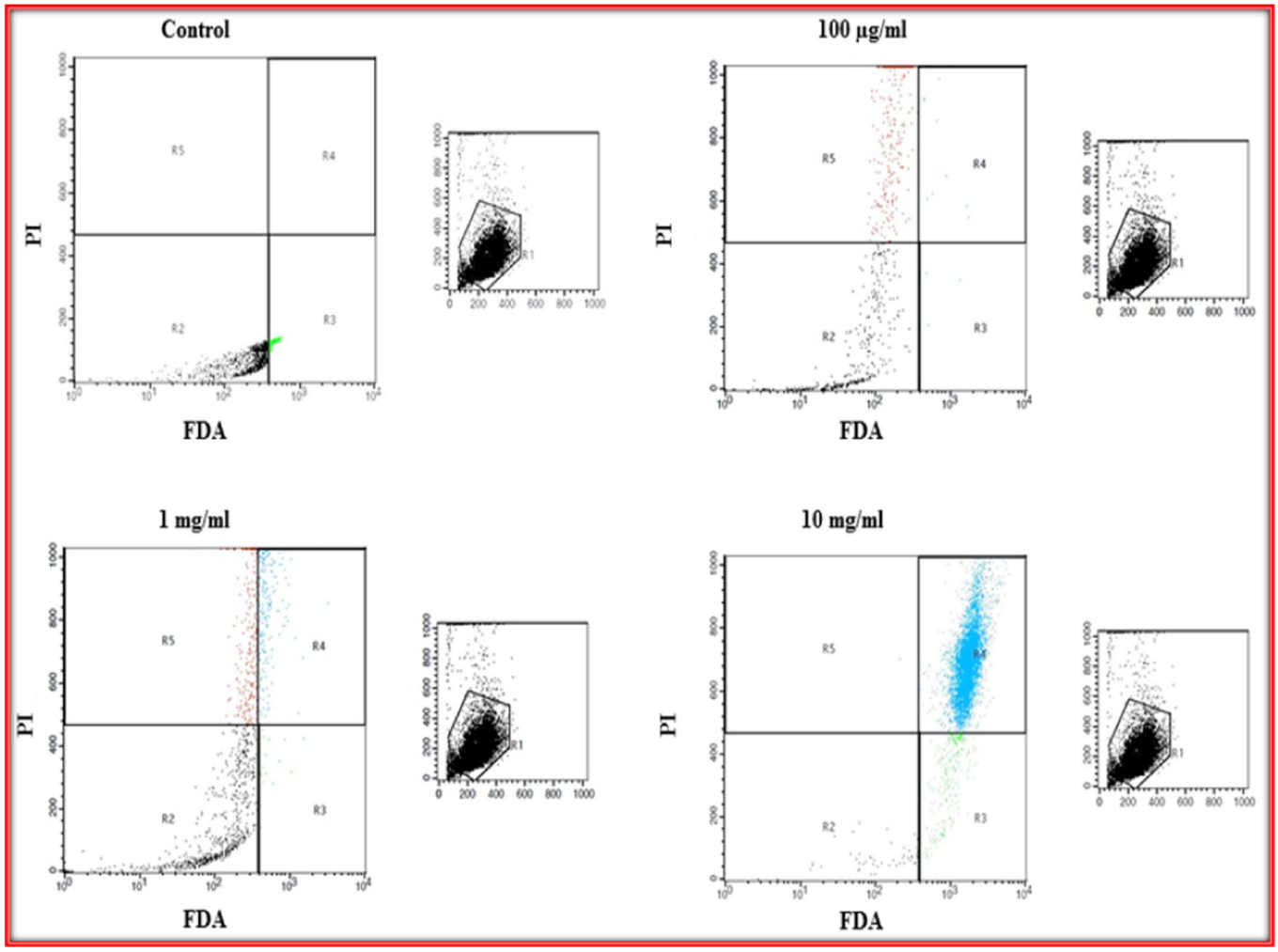

Fig. 6. Effect of CdO nanostructures on Caki-2 cells were determined by FDA and PI. Area R3 is FDA positive, R5 is PI positive, R4 is both FDA and PI positive, and R2 is both FDA and PI negative. The effect of CdO nanostructures (100 µg/ml, 1 mg/ml and 10 mg/ml) on Caki-2 cell was examined at 48 h. The percentage of apoptotic cells were calculated (c).

The physico-chemical properties of the CdO powders were examined by XRD, FTIR, EDAX, XPS, and HR-TEM. The grain-size of the nanostructures was in the range, 20 to 70 nm, which is applicable for biological systems. These results confirmed that the CdO nanostructures were toxic at high doses to both Caki-2 and MDCK cells. Considering the toxic impacts of CdO nanostructure, it is suggested that proper attention be paid before releasing such nano-dimension particles into the environment (in the form of industrial waste) to avoid unnecessary inhalation/direct contact to the humans.

Acknowledgement

This study was supported by the National Research Foundation of Korea (NRF) grant funded by the Korea government (MSIP) (NRF-2014R1A2A1A11052391) and the Nano Material Technology Development Program (2012M3A7B4049675). This study was supported KU-Research Professor Program, Konkuk University, Seoul, South Korea.

References

[1] R. Feynman, There's plenty of room at the bottom, Science 254 (1991) 1300.
[2] J.L. Blum, J.Q. Xiong, C. Hoffman, J.T. Zelikoff, Cadmium associated with inhaled cadmium oxide nanoparticles impacts fetal and neonatal development and growth, Toxicol. Sci. 126 (2012) 478–486.
[3] S. Sharifi, S. Behzadi, S. Laurent, M. Laird Forrest, P. Stroevee, M. Mahmoudi, Toxicity of nanomaterials, Chem. Soc. Rev. 41 (2012) 2323–2343.
[4] A. Albanese, W.C.W. Chan, Effect of gold nanoparticles aggregation on cell uptake and toxicity, ACS Nano 5 (2011) 5478–5489.
[5] A. Pourmand, M. Abdollahi, Current opinion on nanotoxicology, DARU J. Pharm. Sci. 20 (2012) 95–97.
[6] M. Jennifer, W. Maciej, Nanoparticle technology as a double-edged sword: cytotoxic, genotoxic and epigenetic effects on living cells, J. Biomater. Nanobiotechnol. 4 (2013) 53–63.
[7] B. L'Azou, J. Jorly, D. On, E. Sellier, F. Moisan, J. Fleury-Feith, J. Cambar, P. Brochard, C. Ohayon-Courtès, In vitro effects of nanoparticles on renal cells, Part. Fibre Toxicol. 5 (2008) 1–14.
[8] Z. Chen, H. Meng, G. Xing, C. Chen, Y. Zhao, G. Jia, T. Wang, H. Yuan, C. Ye, F. Zhao, Z. Chai, C. Zhu, X. Fang, B. Ma, L. Wan, Acute toxicological effects of copper nanoparticles in vivo, Toxicol. Lett. 163 (2006) 109–120.
[9] H.L. Karlsson, P. Cronholm, J. Gustafsson, L. Möller, Copper oxide nanoparticles are highly toxic: a comparison between metal oxide nanoparticles and carbon nanotubes, Chem. Res. Toxicol. 21 (2008) 1726–1732.
[10] Sk.T. Hossain, S.K. Mukherjee, CdO nanoparticle toxicity on growth, morphology and cell division in *Escherichia coli*, Langmuir 28 (2012) 16614–166122.
[11] R.S. Mane, H.M. Pathan, C.D. Lokhande, S.H. Han, An effective use of nanocrystalline CdO thin films in dye-sensitized solar cells, Sol. Energy 80 (2006) 185–190.
[12] A. Shiori, Jpn. Patent No. 7 (1997) 909.
[13] R. Kondo, H. Okimura, Y. Sakai, Electrical properties of semiconductor photodiodes with semitransparent films, Jpn. J. Appl. Phys. 10 (11) (1971) 1547–1554.
[14] M. Mazaheritehrani, J. Asghari, R. LotfiOrimi, S. Pahlavan, Microwave-assisted synthesis of nano-sized cadmium oxide as a new and highly efficient catalyst for solvent free acylation of amines and alcohols, Asian J. Chem. 22 (4) (2010) 2554–2564.
[15] N.G. Semaltianos, S. Logothetidis, W. Perrie, S. Romani, R.J. Potter, M. Sharp, P. French, G. Dearden, K.G. Watkins, II–VI semiconductor nanoparticles synthesized by laser ablation, Appl. Phys. A Mater. Sci. Process. 94 (2009) 641–647.
[16] A. Heidari, C. Brown, Study of composition and morphology of cadmium oxide (CdO) nanoparticles for eliminating cancer cells, J. Nanomed. Res. 2 (2015) 1–20.
[17] S. Reddy, B.E.K. Swamy, U. Chandra, B.S. Sherigara, H. Jayadevappa, Synthesis of CdO nanoparticles and their modified carbon paste electrode for determination of dopamine and ascorbic acid by using cyclic voltammetry technique, Int. J. Electrochem. Sci. 5 (2010) 10–17.

[18] N. Thovhogi, E. Park, E. Manikandan, M. Maaza, A. Gurib-Fakim, Physical properties of CdO nanoparticles synthesized by green chemistry via *Hibiscus sabdariffa* flower extract, J. Alloys Compd. 655 (2016) 314–320.
[19] P. Muthuraman, G. Enkhtaivan, B. Venkitasamy, B. Mistry, R. Noorzai, B.Y. Jin, D.H. Kim, Time and concentration-dependent therapeutic potential of silver nanoparticles in cervical carcinoma cells, Biol. Trace Elem. Res. 170 (2016) 309–319.
[20] P. Muthuraman, G. Enkhtaivan, D.H. Kim, Cytotoxic effects of aspartame on human cervical carcinoma cells, Toxicol. Res. 5 (2016) 45–52.
[21] K. Anandhan, R. Thilak Kumar, Synthesis, FTIR, UV–Vis and photoluminescence characterizations of triethanolamine passivated CdO nanostructures, Spectrochim. Acta, Part A 149 (2015) 476–480.
[22] J.K. Andeani, S. Mohsenzadeh, Phytosynthesis of cadmium oxide nanoparticles from *Achillea wilhelmsii* flowers, J. Chem. (2013) Article ID 147613. 4 pages.
[23] K.M. Prabu, P.M. Anbarasan, S. Janarthanan, G. Sivakumar, Preparation and characterization of CdO nanoparticles by precipitation method, Int. J. Sci. Res. Dev. 2 (2015) 368–369.
[24] G. Hota, S.B. Ldage, K.C. Khilar, Characterization of nano-sized CdS-Ag_2S core-shell nanoparticles using XPS technique, Colloids Surf. A293 (2007) 5–12.
[25] B. Ramesh, G. Devarajulu, B. Veva Prasad Raju, G. Bhaskar Kumar, G.R. Dillip, A.N. Banerjee, S.W. Joo, Determination of strain, site occupance, photoluminescent, and thermoluminescent-trapping parameters of Sm^{+3}–doped $NaSrB_5O_9$ microstructures, Ceram. Int. 42 (2016) 1234–1245.
[26] L. Huang, J. Yang, X. Wang, J. Han, H. Han, C. Li, Effects of surface modification on photocatalytic activity of CdS nanocrystals studied by photoluminescence spectroscopy, Phys. Chem. Chem. Phys. 15 (2013) 553–560.
[27] J.-C. Dupin, D. Gonbeau, P. Vinatier, A. Levasseur, Systematic XPS studies of metal oxides, hydroxides and peroxides, Phys. Chem. Chem. Phys. 2 (2000) 1319–1324.
[28] J.G. Quiñones-Galván, R. Lozada-Morales, S. Jiménez-Sandoval, Enrique Camps, V.H. Castrejón-Sánchez, E. Campos-González, M. Zapata-Torres, A. Pérez-Centeno, M.A. Santana-Aranda, Physical properties of a non-transparent cadmium oxide thick film deposited at low fluence by pulsed laser deposition, Mater. Res. Bull. 76 (2016) 376–383.
[29] T.V.M. Sreekanth, G.R. Dillip, Yong Rok Lee, *Picrasma quassioides* mediated cerium oxide nanostructures and their post-annealing treatment on the microstructural, morphological and enhanced catalytic performance, Ceram. Int. 42 (2016) 6610–6618.
[30] P. Yeon-Su, O. Yukihiro, K. Noritada, T. Manabu, B. Yosinobu, Aqueous phase-synthesized small CdSe quantum dots: adsorption layer structure and strong band-edge and surface trap emission, J. Nanopart. Res. 13 (2011) 5781–5798.
[31] S. Trilok, D.K. Pandya, R. Singh, Electrochemical deposition and characterization of elongated CdO nanostructures, Mater. Sci. Eng. B 176 (2011) 945–949.
[32] J.M. Moulis, Cellular mechanisms of cadmium toxicity related to the homeostasis of essential metals, Biometals 23 (2010) 877–896.
[33] M. Takagi, H. Satofuka, S. Amano, H. Mizuno, Y. Eguchi, K. Hirata, K. Miyamoto, K. Fukui, T. Imanaka, Cellular toxicity of cadmium ions and their detoxification by heavy metal-specific plant peptides, phytochelatins, expressed in Mammalian cells, J. Biochem. 131 (2002) 233–239.